

Viscoelastic response of sonic band-gap materials

I.E. Psarobas*

*Department of Physics, National Technical University of Athens
Zografou Campus, GR-157 73, Athens, Greece*

(Dated: November 12, 2018)

A brief report is presented on the effect of viscoelastic losses in a high density contrast sonic band-gap material of close-packed rubber spheres in air. The scattering properties of such a material are computed with an on-shell multiple scattering method, properties which are compared with the lossless case. The existence of an appreciable omnidirectional gap in the transmission spectrum, when losses are present, is also reported.

PACS numbers: 43.20.+g; 43.40.+s; 43.35.+d

The problem of elastic wave propagation in inhomogeneous media is of great importance in many branches of physics, mathematics and engineering. In particular, matters such as the localization of classical waves¹ and the formation of spectral gaps in periodic elastic composites,^{2,3} have drawn the attention of researchers over the last decade. In particular, phononic or sonic crystals are composite materials which consist of homogeneous particles (solid or fluid inclusions the dimensions of which are large enough in order for a macroscopic description of their elastic properties to be valid) distributed periodically in a host medium characterized by different mass density and Lamé coefficients. With an appropriate choice of the parameters involved one may obtain sonic crystals with absolute frequency gaps (omnidirectional sonic gaps).

Among the various methods available for the calculation of the elastic properties of phononic crystals, the traditional band-structure methods mainly deal with periodic, infinite, and nondissipative structures. However in an experiment, one deals with finite-size slabs and the measured quantities are, usually, the transmission and reflection coefficients. Apart from that, realistic structures are dispersive and have losses. This limitation of traditional band-structure calculations was noticed in a theoretical study of colloidal crystals with ultrasound.⁴ We remember that a usual band-structure calculation proceeds with a given wave vector, \mathbf{k} , and computes the eigenfrequencies within a wide frequency range together with the corresponding eigenmodes. On the contrary, on-shell methods proceed differently: the frequency is fixed and one obtains the eigenmodes of the crystal for this frequency. These methods are ideal when one deals with dispersive materials (with or without losses). Moreover on-shell methods are computationally more efficient than traditional band-structure methods.⁵ Psarobas *et al.* have recently developed an on-shell method for phononic crystals,⁶ which applies to systems which consist of nonoverlapping homogeneous spherical particles arranged periodically in a host medium characterized by different elastic coefficients. The method provides the complex band structure of the infinite crystal associated with a given crystallographic plane; and also the transmission, reflection, and absorption coefficients

of an elastic wave incident at any angle on a slab of the crystal, parallel to a given plane, of finite thickness.

The present work introduces the effect of viscoelasticity in a sonic band-gap material. For this purpose, a binary system of close-packed rubber spheres in air is chosen. The viscoelastic response of the system is accounted for by means of the Kelvin-Voigt model,⁷ which is well-suited for materials and ultrasonic frequencies of major interest. The problem of acoustic-wave scattering by a single viscoelastic sphere of radius S has been adequately addressed in the past⁷ according to the Kelvin-Voigt viscoelastic model. In such a case the sphere is considered to be elastic with modified shear and compressional complex wavenumbers, the imaginary parts of which represent a measure of the loss. In particular, for an absorbing sphere in an inviscid fluid background, the complex compressional and shear wavenumbers are conveniently defined as

$$\begin{aligned} q_{sl} &= \frac{c_l}{c_{sl}} \frac{q_l}{\sqrt{1 - i[(\alpha + \beta)/\rho_s c_{sl}^2]}}, \\ q_{st} &= \frac{c_l}{c_{st}} \frac{q_l}{\sqrt{1 - i(\beta/\rho_s c_{st}^2)}}, \end{aligned} \quad (1)$$

where $q_l = \omega/c_l$ refers to the fluid environment with ω being the angular frequency and c_l the respective speed of sound. The real parts of the complex Lamé parameters of the sphere, $\lambda_s = \lambda_{se} - i\lambda_{sv}$ and $\mu_s = \mu_{se} - i\mu_{sv}$, combined with the density ρ_s yield the compressional and shear wave speeds respectively

$$c_{sl} = \sqrt{(\lambda_{se} + 2\mu_{se})/\rho_s}, \quad c_{st} = \sqrt{\mu_{se}/\rho_s}. \quad (2)$$

The imaginary parts of the Lamé parameters are connected to the viscous losses $\alpha + 2\beta$, and β of the sphere as follows: $\alpha = \omega\lambda_{sv}$, $\beta = \omega\mu_{sv}$. The problem of elastic scattering by a solid sphere in an inviscid fluid¹¹ is described by the scattering transition matrix, the elements of which, in the angular momentum representation (l, m) (see Appendix), connect the spherical wave expansion coefficients⁶ of the scattered field to those of the incident.

Multiple scattering effects within planes of spheres, sonic crystals and slabs of the same are taken into account by the method described in Ref. 6. This method views the crystal as a sequence of planes of spheres parallel to

a given surface: a crystallographic plane described by a two-dimensional (2D) lattice $\{\mathbf{R}_n\}$. The corresponding 2D reciprocal lattice we denote by $\{\mathbf{g}\}$. In the host region between the n -th and the $(n+1)$ -th planes, a Bloch wave solution for the displacement field (harmonic time dependence is assumed), corresponding to a given frequency ω and a given reduced wave vector \mathbf{k}_{\parallel} within the surface Brillouin zone (SBZ) of the given surface, can be expanded into plane waves propagating (or decaying) to the left and to the right, as follows:

$$\mathbf{u}(\omega; \mathbf{k}_{\parallel}) = \sum_{\mathbf{g}} \left\{ \mathbf{u}_{\mathbf{g}n}^{+} \exp \left[i \mathbf{K}_{\mathbf{g}l}^{+} \cdot (\mathbf{r} - \mathbf{A}_n) \right] + \mathbf{u}_{\mathbf{g}n}^{-} \exp \left[i \mathbf{K}_{\mathbf{g}l}^{-} \cdot (\mathbf{r} - \mathbf{A}_n) \right] \right\}, \quad (3)$$

where

$$\mathbf{K}_{\mathbf{g}l}^{\pm} = \left(\mathbf{k}_{\parallel} + \mathbf{g}, \pm \left[(\omega/c_l)^2 - (\mathbf{k}_{\parallel} + \mathbf{g})^2 \right]^{1/2} \right) \quad (4)$$

and \mathbf{A}_n is a point between the n th and $(n+1)$ th planes. We note that the separation of two successive planes of spheres need only be larger than the radii of the spheres of the two planes (see pg. 86 of Ref. 8). It should be also noted that, although both shear and compressional modes are considered within the spheres and enter the calculation through the scattering transition matrix (see Appendix), only longitudinal waves exist in the host (air) region [see Eq. (3)]. As a consequence of that, in a binary composite of nonoverlapping solid spheres in a fluid host, such as the one being investigated in this report, there are no propagating shear waves if the solid component does not form a continuous network.

A generalized, i.e. propagating or evanescent, Bloch wave satisfies the equation

$$\mathbf{u}_{\mathbf{g}n+1}^{\pm} = \exp(i\mathbf{k} \cdot \mathbf{a}_3) \mathbf{u}_{\mathbf{g}n}^{\pm}, \quad (5)$$

where $\mathbf{a}_3 = \mathbf{A}_{n+1} - \mathbf{A}_n$ and $\mathbf{k} = (\mathbf{k}_{\parallel}, k_z(\omega; \mathbf{k}_{\parallel}))$ is the Bloch wavevector. There are infinitely many such solutions for given \mathbf{k}_{\parallel} and ω , corresponding to different values of the z -component, $k_z(\omega; \mathbf{k}_{\parallel})$, of the reduced wave vector \mathbf{k} , but in practice one needs to calculate only a finite number (a few tens at most) of these generalized Bloch waves. We have propagating waves [for these $k_z(\omega; \mathbf{k}_{\parallel})$ is real] which constitute the normal modes of the infinite crystal; and evanescent waves [for these $k_z(\omega; \mathbf{k}_{\parallel})$ is imaginary] which do not represent real waves, but they are useful mathematical entities which enter into the evaluation of the reflection and transmission coefficients of a wave, with the same ω and \mathbf{k}_{\parallel} , incident on a slab of the crystal parallel to the given surface. The transmission/reflection matrices for a slab which consists of a stack of layers of spheres with the same 2D periodicity parallel to a given plane of the crystal are obtained from the transmission/reflection matrices of the individual layers in the manner described in Ref. 6. Knowing the transmission/reflection matrices for the slab we can

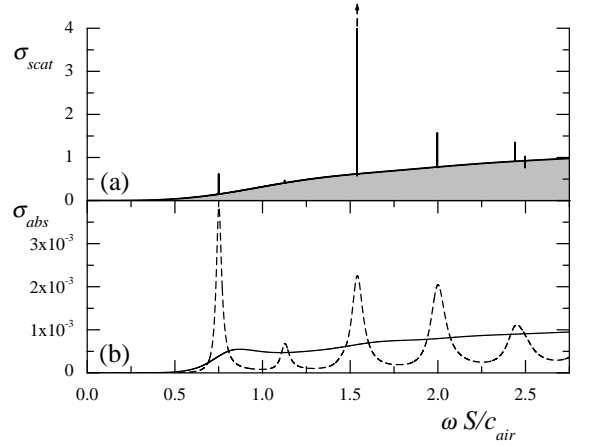


FIG. 1: (a): Normalized total scattering cross section of a rubber sphere in air. The solid line corresponds to a sphere with no losses and the shaded curve to a sphere with losses. The two different viscous levels used here, for the sphere, are hardly distinguishable. The resonance with the arrow extends twice as high. (b): Normalized absorption cross section of a viscoelastic rubber sphere. The dotted (solid) line corresponds to the low (high) viscous level used here.

readily obtain the transmission, reflection, and absorption coefficients of a plane acoustic wave incident on the slab.

The system which will be examined here is a crystal of rubber spheres in air. The physical parameters entering our calculations are taken from Ref. 7. In particular, the mass density of air is $\rho_{air} = 1.2 \text{ kg/m}^3$ and its respective speed of sound $c_{air} = 334 \text{ m/s}$. The rubber spheres have a mass density $\rho_s = 1130 \text{ kg/m}^3$ and $c_{ls} = 1400 \text{ m/s}$, $c_{ts} = 94 \text{ m/s}$ are the compressional and shear speeds of sound, respectively. In addition, according to Ref. 7, three different viscoelastic levels are considered for the rubber spheres, namely: lossless spheres ($\alpha = \beta = 0$), a low viscous level ($\alpha_{low} = 0.5 \text{ MPa/s}$, $\beta_{low} = 0.01 \text{ MPa/s}$) and a high viscous level ($\alpha_{high} = 5 \text{ MPa/s}$, $\beta_{high} = 0.1 \text{ MPa/s}$). The viscoelastic properties used in this study are typical values for commercial rubbers, the variety of which is quite extensive⁹ and frequency dependent at high ultrasonic frequencies.¹⁰

Before dealing with the main object of this work, it will be useful to state briefly certain basic features of the acoustic scattering problem by a viscoelastic sphere.⁷ These features will be used extensively in what follows. These are presented in Fig. 1, obtained with an angular momentum cutoff, $l_{max} = 5$, which yields an accuracy of better than 0.001% in the given frequency range. On first sight, one may observe the disappearance of the sharp modal resonances in the scattering cross section of the sphere (see Appendix), when viscoelasticity is turned on. Also, there is no significant difference between the two viscous levels (low and high) in scattering. On the contrary absorption (see Appendix) seems to be different for the two cases. The low viscous level induces resonant ab-

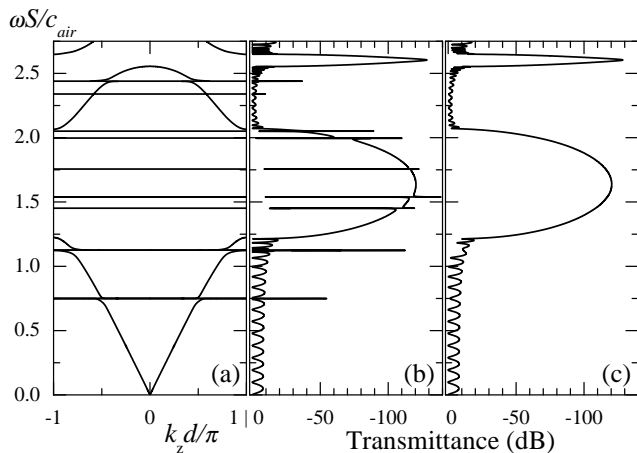


FIG. 2: The sonic band structure at the center of the SBZ of a (111) surface of an fcc crystal of close-packed lossless rubber spheres in air (a). The corresponding transmittance curve of a slab of 16 layers parallel to the same surface is given in (b). In (c) the same transmittance curve is presented but with spheres of the low viscous level. d is the distance between successive (111) planes of the fcc crystal under consideration.

sorption exactly at the resonant frequencies of the lossless case, while the higher viscous level washes everything out as if there was no inner resonant structure in the system.

We next consider an fcc crystal of close-packed (almost touching) rubber spheres in air. We view the crystal as a succession of planes of spheres parallel to the (111) fcc surface. Fig. 2(a) shows the frequency band structure normal to the fcc (111) plane ($\mathbf{k}_{\parallel} = \mathbf{0}$) and the corresponding transmission spectrum for waves incident normally on a slab of the crystal consisting of 16 layers of lossless spheres. The results are obtained with an angular momentum cutoff $l_{max} = 7$ and 55 \mathbf{g} vectors (the established convergence is within an accuracy of better than a tenth of a percent). One observes, besides a large Bragg gap extending from $\omega S/c_{air} = 1.223$ to $\omega S/c_{air} = 2.065$, a number of flat bands which derive from the interacting sharp resonant modes localized on the individual rubber spheres (see Fig. 1). Because these bands are so narrow in the present case, they are hardly observable; except that they introduce small gaps, above and below the main gap, which result from the hybridization of these flat bands with the broad bands corresponding to nearly free propagating waves. These narrow gaps are seen more clearly in the transmission spectrum [Fig. 2(b)]. Within the main gap these flat bands manifest themselves as sharp peaks in the transmission spectrum. The long wavelength limit is represented by the linear segments of the dispersion curves of Fig. 2(a), the slopes of which determine the propagation velocity of acoustic waves ($\bar{c}_l = 1.54 c_{air}$) in a corresponding effective medium. The oscillations in the transmission coefficient, over the allowed regions of frequency, are due to interference effects resulting from multiple reflection at the surfaces of the slab of the crystal (Fabry-Pérot-type oscillations). When losses are present

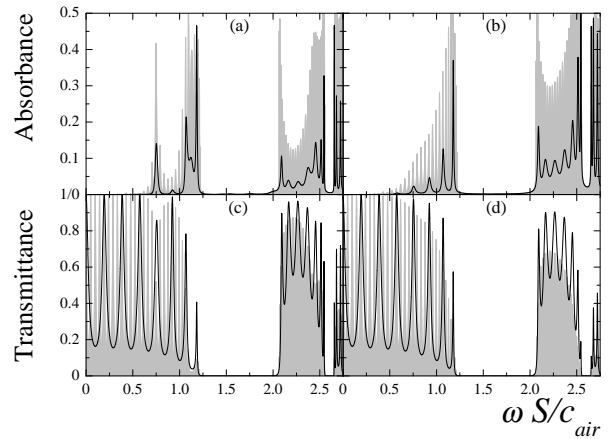


FIG. 3: Absorbance and transmittance curves of slabs of the rubber sonic crystal described in Fig. 2(a) consisting of 8 [(a),(c)] and 32 [(b),(d)] planes of spheres, respectively. The black line (shaded curve) corresponds to the low (high) viscous level.

in the system, there are no true propagating waves and the band structure of the infinite lossless crystal is not of any help, therefore the effect of the low viscous level is shown in the transmission spectrum [Fig. 2(c)]. As expected from the results of the single sphere, the sharp peaks and dips of the resonant states disappear and we obtain a “clean” sonic gap without any resonant modes within it. The existence of the frequency gap means that sound does not propagate through the crystal when its frequency lies within the gap (the intensity of the wave decays exponentially into the crystal for these frequencies), and if it cannot enter into the crystal, it cannot be absorbed either. This is shown in Fig. 3.

The close relation between absorption and transmission is demonstrated in Fig. 3 for slabs consisting of 8 and 32 (111) planes of spheres, and for normal incidence. The solid lines correspond to the lower viscous level and the shaded curves to the higher one. A relatively large transmission coefficient implies that a correspondingly large fraction of sound has gone through the slab, with a consequent higher probability of being absorbed. However, since losses are due to the rubber spheres, absorption mainly occurs about the frequency regions where the modes of the acoustic field are mostly localized in the spheres. This explains why, outside the gap regions, absorption takes place essentially about the frequencies of the flat bands.

In Fig. 4, the projection of the frequency band structure on the SBZ of the (111) plane of the fcc crystal along its symmetry lines is shown. This is obtained, for a given \mathbf{k}_{\parallel} , as follows: the regions of frequency over which there are no propagating states in the infinite crystal [the corresponding values of all $k_z(\omega, \mathbf{k}_{\parallel})$ are complex] are shown in white, against the shaded areas which correspond to regions over which propagating states do exist [for a given ω there is at least one solution corresponding to $k_z(\omega, \mathbf{k}_{\parallel})$].

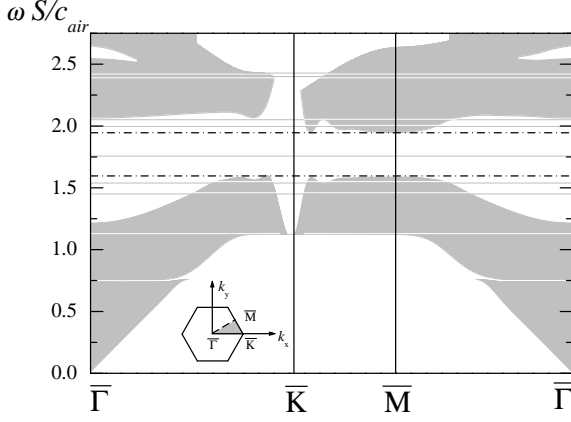


FIG. 4: Projection of the frequency band structure on the SBZ of the (111) surface of the fcc sonic crystal described in the caption of Fig. 2. The white areas show the frequency gaps in the considered frequency region. The broken lines map the omnidirectional frequency gap in the transmission spectrum of a slab of the crystal, with losses, of finite thickness. Finally, the inset shows the SBZ of the fcc (111) surface.

real]. One clearly sees here how the resonances on spheres lead to narrow hybridization gaps above and below the main gap, and flat bands in the gap regions. When losses are present, the crystal under investigation exhibits an appreciable omnidirectional sonic transmission gap extending from $\omega S/c_{air} = 1.595$ up to 1.946. Finally, we note that the results obtained depend on the ratio λ_0/S (λ_0 is the wavelength of the incident sound wave) and are therefore applicable over different ranges of frequencies, provided that the viscoelastic properties of the spheres do not vary significantly with the frequency.

Acknowledgments

This work has been supported by the Institute of Communication and Computer Systems (ICCS) of the National Technical University of Athens. Support from the University of Athens is also acknowledged.

APPENDIX A

Applying the proper boundary conditions at the interface between the surrounding fluid and the sphere,¹¹ requiring the continuity of the radial component of the displacement field and the surface traction, along with

the requirement that there is no tangential component of the surface traction at the interface, we can determine the scattering matrix which connects the incident with the scattered field. Here for reasons of completeness, along the lines of the formalism established in Ref. 6, the nonzero elements of the \mathbf{T} matrix for a solid sphere in a fluid host are

$$T_{lm;l'm'}^{LL} = \frac{W_l^{LL}}{D_l} \delta_{ll'} \delta_{mm'}, \quad l, l' \geq 0, \quad (\text{A1})$$

with $z_l = Sq_l$ referring to the fluid and $x_\nu = Sq_{s\nu}$, with $\nu = l, t$ to the sphere. The superscripts LL refer to the case of scattering in a fluid host, since incident and scattered waves are L -type compressional waves. The 3×3 determinants D_l and W_l^{LL} are given by

$$D_l = \begin{vmatrix} d_{22} & d_{23} & d_{24} \\ d_{32} & d_{33} & d_{34} \\ d_{42} & d_{43} & d_{44} \end{vmatrix}, \quad W_l^{LL} = - \begin{vmatrix} d_2^L & d_{23} & d_{24} \\ d_3^L & d_{33} & d_{34} \\ d_4^L & d_{43} & d_{44} \end{vmatrix} \quad (\text{A2})$$

where

$$\begin{aligned} d_{22} &= z_l h_l^{+'}(z_l), \quad d_{23} = l(l+1)j_l(x_t), \quad d_{24} = x_l j_l'(x_l), \\ d_{32} &= 0, \quad d_{33} = [l(l+1) - 1 - x_t^2/2] j_l(x_t) - x_t j_l'(x_t), \\ d_{34} &= x_l j_l'(x_l) - j_l(x_l), \quad d_{42} = -x_t^2 \rho h_l^+(z_l)/(2\rho_s), \\ d_{43} &= l(l+1)[x_t j_l'(x_t) - j_l(x_t)], \\ d_{44} &= [l(l+1) - x_t^2/2] j_l(x_l) - 2x_l j_l'(x_l), \\ d_2^L &= z_l j_l'(z_l), \quad d_3^L = 0, \quad d_4^L = -x_t^2 \rho j_l(z_l)/(2\rho_s). \end{aligned} \quad (\text{A3})$$

j_l' and $h_l^{+'}$ denote the first derivatives of the spherical Bessel and Hankel functions, respectively. The \mathbf{T} matrix, because of spherical symmetry is diagonal in l and independent of m .

The exact form of the above \mathbf{T} matrix allows us to compute the normalized total scattering cross section of an elastic sphere (scattering cross section over πS^2) in a fluid host,

$$\sigma_{total} = \frac{4}{z_l^2} \sum_{l=0}^{\infty} (2l+1) |T_{lm;lm}^{LL}|^2. \quad (\text{A4})$$

In addition the normalized absorption cross section is given by

$$\sigma_{abs} = -\frac{4}{z_l^2} \sum_{l=0}^{\infty} (2l+1) \left\{ |T_{lm;lm}^{LL}|^2 + \text{Re}[T_{lm;lm}^{LL}] \right\}. \quad (\text{A5})$$

* Also at the Section of Solid State Physics of the University of Athens, Panepistimioupolis, GR-157 84, Athens, Greece.; Electronic address: ipsarob@cc.uoa.gr; URL: <http://www.uoa.gr/~vyannop>

¹ *Scattering and Localization of Classical Waves in Random Media*, edited by P. Sheng (World Scientific, Singapore, 1990); P. Sheng, *Introduction to Wave Scattering, Localization and Mesoscopic Phenomena* (Academic Press, San Diego, 1995).

- ² M. M. Sigalas, and E. N. Economou, J. Sound Vib. **158**, 377 (1992).
- ³ M. S. Kushwaha, P. Halevi, L. Dobrzynski, and B. Djafari-Rouhani, Phys. Rev. Lett. **71**, 2022 (1993).
- ⁴ R. Sprik and G.H. Wegdam, Solid State Commun. **106**, 77 (1998).
- ⁵ Y. Qiu, K.M. Leung, L. Carin, and D. Kralj, J. Appl. Phys. **77**, 3631 (1995).
- ⁶ I. E. Psarobas, N. Stefanou, and A. Modinos, Phys. Rev. B **62**, 278 (2000).
- ⁷ V. M. Ayres and G. C. Gaunard, J. Acoust. Soc. Am. **81**, 301 (1987).
- ⁸ A. Modinos, *Field, Thermionic and Secondary Electron Emission Spectroscopy* (Plenum Press, New York, 1984).
- ⁹ Quick search by material name: “rubber”, at <http://www.matweb.com> .
- ¹⁰ <http://www.ultrasonic.com/tables/rubbers.htm>
- ¹¹ D. Brill and G. Gaunard, J. Acoust. Soc. Am. **81**, 1 (1987).